Synthesis and Characterization of Bisphenol-C Epoxy Crotonate and Its Fiber-Reinforced Composites

PARSOTAM H. PARSANIA*[1], JIGNESH V. PATEL[2] AND JIGNESH P. PATEL[3]

[1,2,3]*Polymer Chemistry Division, Department of Chemistry, Saurashtra University, Rajkot, Gujarat, India*

ABSTRACT

Bisphenol-C epoxy crotonate resin was synthesized by reacting 8.09g epoxy resin of bisphenol-C, and 2.15g crotonic acid using 25 mL 1,4-dioxane as a solvent, and 1 mL triethylamine as a catalyst at reflux temperature for 1-6 h. Solid epoxy crotonate (ECCR) is highly soluble in common organic solvents. ECCR was characterized by its acid (24.5-1.5 mg KOH/g) and hydroxyl (504.5-678.4 mg KOH/g) values. The structure of ECCR is supported by FTIR and ^{1}HNMR spectroscopic methods. A DSC endothermic transition at 229^{o}C indicated melting followed by thermal polymerization of ECCR. ECCR is thermally stable up to 320^{o}C and follows three-step degradation kinetics. The first step followed first-order degradation kinetics, while the second and third steps followed one-half-order degradation kinetics. High values of kinetic parameters suggested the rigid nature of the crosslinked resin. Jute-, Glass- and Jute-natural fiber-ECCR composites showed moderate tensile strength, flexural strength, electric strength, and volume resistivity due to the rigid nature and poor interfacial adhesion of the composites. J-ECCR and G-ECCR composites showed high water absorption tendency and excellent hydrolytic stability against water, 10% aq. HCl and 10% aq. NaCl and even in boiling water. Mechanical and electrical properties and water absorption tendency of the composites indicated their usefulness as low load-bearing housing and insulating materials. They can also be utilized in harsh environmental conditions.

KEYWORDS: *Bisphenol-C epoxy crotonate, Acid and hydroxyl values, FTIR, ^{1}HNMR, DSC, TGA, Composites, Water absorption.*

J. Polym. Mater. Vol. **40,** No. 3-4, 2023, 271-284

*Correspondence author e-mail: phparsania22@gmail.com and phparsania@aol.com
DOI : https://doi.org/10.32381/JPM.2023.40.3-4.9

INTRODUCTION

Vinyl ester, epoxy, and unsaturated polyester resins are well-known as high-performance matrices and are most widely useful in microelectronics, automotive, aerospace, building construction, furniture, paint, and marine industries[1-4]. Vinyl ester resins (VERs) have emerged as promising matrices with higher design flexibility, room temperature curing, easy processing of desired thermal and mechanical properties, low water absorption tendency, and excellent chemical, corrosion, fire, and heat resistance[5]. Because of these properties, VERs are most widely used in coatings, adhesives, molding compounds, structural laminates, and electrical and marine components. They are mainly used in manufacturing tanks, ducts, pipes, automobiles, and scrubbers[6].

Ethenically unsaturated carboxylic acids wherein α-alkyl substituent consisting of 1-4 carbon atoms are used in the syntheses of VERs but most preferably methacrylic acid is used. VERs contain reactive terminal ester groups, which are less susceptible to hydrolysis than those in unsaturated polyester resins and contribute to the excellent chemical resistance of the cured products. The epoxy backbone of VERs imparts toughness to the cured films, while the carbon-carbon and ether bonds improve the chemical resistance. The hydroxyl groups of VERs increase the polarity, which can improve the wettability of the adhesive.

Globally various natural fibers like jute, bamboo, coconut, kenaf, ramie, rice, sugar cane, pineapple, and many more are available in abundance. These fibers are extracted from various parts of the plants (stems, leaves, fruits, seeds, and husks) by different methods[7]. They are used in making many traditional items and also in fiber-reinforced composites, which are alternatives to plywood. Various plant fibers such as bamboo, coconut, kenaf, ramie, nettles, abaca, pineapple, sugar cane, rice, and grass are used for the production of fiber-reinforced composites. The main limitations of natural fibers over synthetic inorganic fibers (glass, carbon, alumina, and wollastonite fibers) are their high water absorption and flammability.

A literature survey on syntheses, physicochemical properties as well as fiber-reinforced composites of VERs revealed that most of the investigators have used readily commercially available bisphenol-A-based epoxy vinyl ester resins and very few researchers have worked on epoxy vinyl esters based on other bisphenols[8-19]. In our laboratory, we have synthesized and characterized bisphenol-C epoxy VERs and used them for synthetic and natural fiber-reinforced composites, and evaluated their performances[13-19]. We achieved good mechanical and electrical properties as well as excellent chemical resistance against different environmental conditions. The present research work deals with the synthesis and characterization of bisphenol-C epoxy crotonate is utilized to fabricate different natural fiber-reinforced composites. The performance of the composites is evaluated by determining their mechanical and electrical properties, and chemical resistance against water, 10% aq. acid and 10% aq. saline solutions at room temperature as well as in boiling water.

EXPERIMENTAL

Materials and Methods

Laboratory-grade solvents and chemicals are used either as received or purified wherever necessary before their use. Epoxy resin of bisphenol-C (EBC) having EEW 809 was used in the present work. Crotonic acid, styrene, triethylamine, hydroquinone, chloroform, acetone, DMF, DMSO, THF, methyl ethyl ketone, and 1, 4-dioxane, were supplied by Spectro Chem, Mumbai. Woven jute fabric (Brown jute, Corchorus capsularis) used in the present work was purchased from the local market (Rajkot) and silane-treated E-glass fabric (7 mils) was purchased from Unnati Chemicals, India Ahmedabad. Methyl ethyl ketone peroxide (MEKP) and 6% cobalt naphthenate were furnished by EPP Composites, Rajkot as free samples and were used as received. Some of the locally available natural fibers namely banana fiber, sugarcane husk, coir fiber, wheat husk, and groundnut shells were collected either from the local market or farms. Jute and glass fibers are aligned vertically and horizontally in the fabrics. Jute fabric was dried at 60°C for 3 h before its use. Collected natural fibers were cleaned, dried, chopped (2-3 mm), and stored in airtight containers.

Synthesis of bisphenol-C epoxy-crotonate Resin

Two neck round-bottomed flask was equipped with a mechanical stirrer and a condenser was placed into a water bath. To this flask, 8.09g EBC, 25 mL 1,4-dioxane, 2.15g crotonic acid, and 1 mL triethylamine catalyst were transferred, and the mixture was stirred at room temperature for 5 min. The reaction mass was brought to reflux with stirring continued up to 1h and cooled to room temperature. Solid epoxy crotonate was isolated from the excess cold water, filtered, washed well with a bicarbonate solution till unreacted acid was removed, and finally washed with distilled water and dried in an oven at 50°C. Similarly, esterification reactions were carried out for up to 6h by fixing a 1h reaction time interval. Epoxy crotonate was found highly soluble in common organic solvents like chloroform, acetone, DMF, DMSO, THF, methyl ethyl ketone, 1, 4-dioxane, etc. Epoxy crotonate samples were purified three times dissolving in 1,4-dioxane and precipitating in a large excess of water and designated as ECCR.

The acid and hydroxyl values of ECCR samples were determined in triplicate and mean values are reported in Table 1 from which it is observed that acid value decreased and hydroxyl value increased with reaction time. A very low acid value of 1.5mg KOH/g indicated the completion of the esterification reaction. The required acid values (< 30) were achieved within a 1 h reaction time. Following 1h reaction time, the bulk quantity of ECCR was synthesized. A 50% ECCR was prepared in styrene as a reactive diluent and 0.2% hydroquinone was added as an inhibitor. The reaction scheme is shown below.

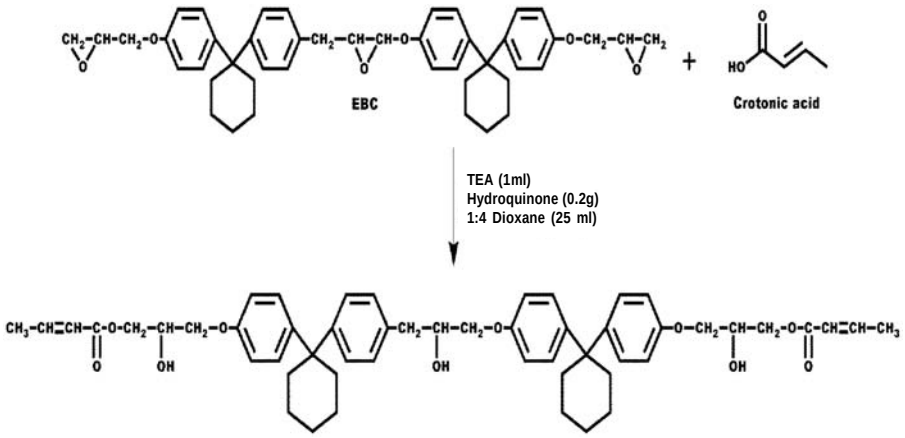

Scheme-I: Synthesis of bisphenol-C epoxy crotonate (ECCR)

TABLE 1: Acid and hydroxyl values of ECCR

Reaction time, h	1	2	3	4	5	6
Acid value, mg KOH/g	24.5	19.9	15.2	9.9	4.7	1.5
Hydroxyl value, mg KO/g	504.5	574.6	602.2	623.7	664.9	678.4

Fabrication of Composites

Jute/Glass/Jute-natural fiber reinforced composites were prepared by hand layup compression molding technique. A 1% of methyl ethyl ketone peroxide (MEKP) and 1% of cobalt naphthenate of ECCR were used as an initiator and as a promoter, respectively. In sandwich composites, the jute-to-biomass ratio was kept at 1:2. The experimental details are given in Table 2. Required quantities of ECCR, MEKP, and promoter were dissolved in 100-130 mL chloroform and the resultant solution was applied to 21cm X 21cm jute or glass fabric with a smooth brush. The prepregs were dried in sunlight for about 15 min. Eight jute or ten glass prepregs were stacked one over the other and pressed between two preheated stainless steel plates under hydraulic pressure of 20 Bar at 110°C for 5h. Silicone spray was used as a mold-releasing agent. Similarly, jute-biomass sandwich composites of sugarcane (SC)/banana (B)/ coir (CO) /wheat husk (WH)/groundnut (GN) shell fibers were prepared. The first two jute sheets were impregnated with ECCR solution and then after 1-2 mm chopped natural fibers were mixed thoroughly and dried in sunlight. The impregnated biomass was sandwiched uniformly between two impregnated jute sheets and pressed as stated above. The required size samples were machined according to standard test methods. Jute and glass composites are abbreviated as J-ECCR and G-ECCR, respectively. Similarly, sandwich composites are abbreviated as J-B-ECCR, J-SC-ECCR, J-CO-ECCR, J-WH-ECCR, and J-GN-ECCR.

TABLE 2: Experimental details for the fabrication of jute/glass/jute-biomass-ECCR composites

Composite	Wt. of jute/glass fabric, g	Wt. of biomass, g	ECCR, g
J- ECCR	158	-	111
G-ECCR	115	-	81
J-B- ECCR	43	86	129
J-SC- ECCR	44	88	132
J-CO- ECCR	41	82	123
J-WH- ECCR	39	78	117
J-GN- ECCR	41	82	123

Materials Characterization

IR (KBr pellet) and ^{1}HNMR spectral analyses of ECCR were carried out on a Shimadzu FTIR-8400 spectrometer and a Brucker FTNMR (300 MHz) spectrometer, respectively. In ^{1}HNMR spectral analysis, $CDCl_3$ was used as a solvent, and TMS as an internal standard. Differential scanning calorimetric (DSC) and thermogravimetric (TG) measurements at the 10 °C min^{-1} heating rate and in a nitrogen atmosphere were made on a Shimadzu DSC-60 and Shimadzu DTG-60H, respectively. The tensile strength (ISO/R 527-1996 Type-I), and flexural strength (ASTM-D-790-2003) measurements were performed on a Shimadzu Autograph Universal Tensile Testing Machine, Model No. AG-X Series at a speed of 10 mm min^{-1}. The electric strength (IEC-60243-Pt-1-1998) measurements were carried out on a high voltage tester (Automatic Electric-

Mumbai) in the air at 27°C by using 25/75mm brass electrodes. Volume resistivity (ASTM-D-257-2007) measurements were made on a Hewlett Packard high resistance meter in the air at 25°C after charging for 60 sec at 500 V DC applied voltage. Each of the samples was tested 3-5 times and average values were considered. Water absorption in J-ECCR and G-ECCR against distilled water, 10% aqueous HCl, and 10% aqueous NaCl solutions and also in boiling water was carried out by the change in mass method at 35°C according to our recent publication[16].

RESULTS AND DISCUSSION

Spectral Analysis

IR spectrum of ECCR is presented in Fig.1. Observed characteristic absorption peaks (cm^{-1}) are 3435.3 (-OH str.), 2933.8 (C-H, asym. str.), 2858.6 (C-H, sym. str.), 1712.9 (C=O, str.), 1606.8, 1510.3 and 1448.6 (C=C str.), 1244.1 (C-O-C str.) besides aromatic C-H in-plane and out of plane deformation vibrations. Thus, IR peaks supported the presence of functional groups present in ECCR.

^{1}HNMR spectrum of ECCR is presented in Fig. 2. Chemical shifts (ppm) and multiplicities of the peaks are assigned as follows. The signal at 1.441-1.399 (m, $\beta+\gamma$ –CH_2- of cyclohexyl ring), 1.799-1.779 (d, -CH_3), 2.120 (s, α –CH_2- of cyclohexyl ring), 3.621-3.595 (m, -CH-OH), 3.686-3.664 (m, -CH_2O), 3.884-4.002 (m, -OCH_2), 4.238-4.210 (m, -CH-OH), 5.811-5.769 (dd, -CH=CH-), 6.735-6.714 (d, ArH), 7.087-7.059 (m, ArH). Residual solvent and water appeared at 7.181 and 2.48 ppm, respectively. ^{1}HNMR supported expected protons in the resin molecule. Thus, IR and ^{1}HNMR spectral data confirmed the structure of ECCR.

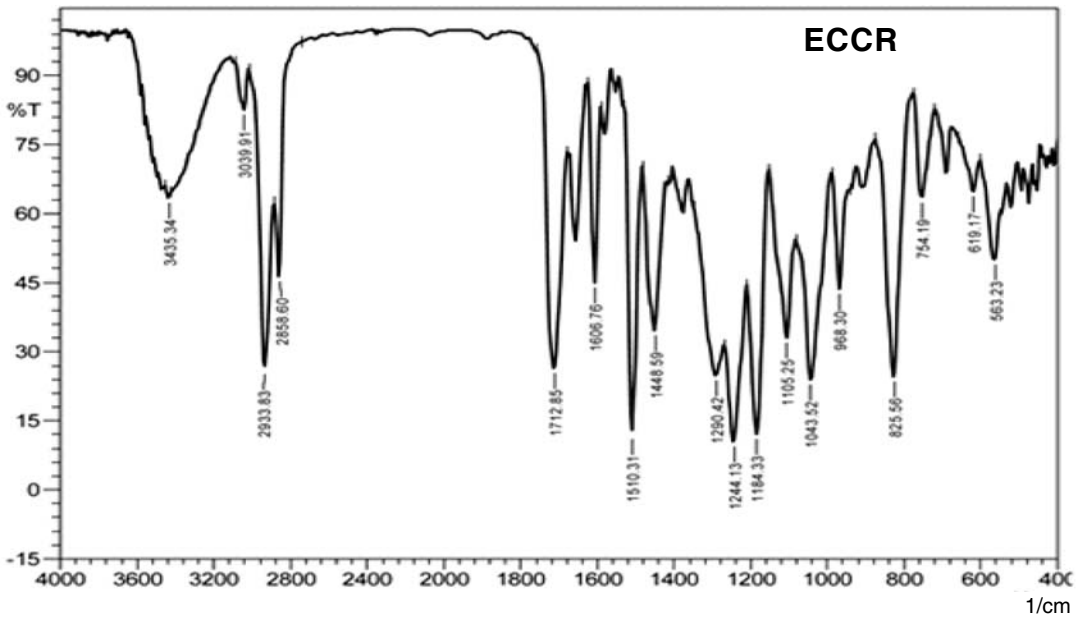

Fig. 1. FTIR spectrum (KBr pellet) of ECCR.

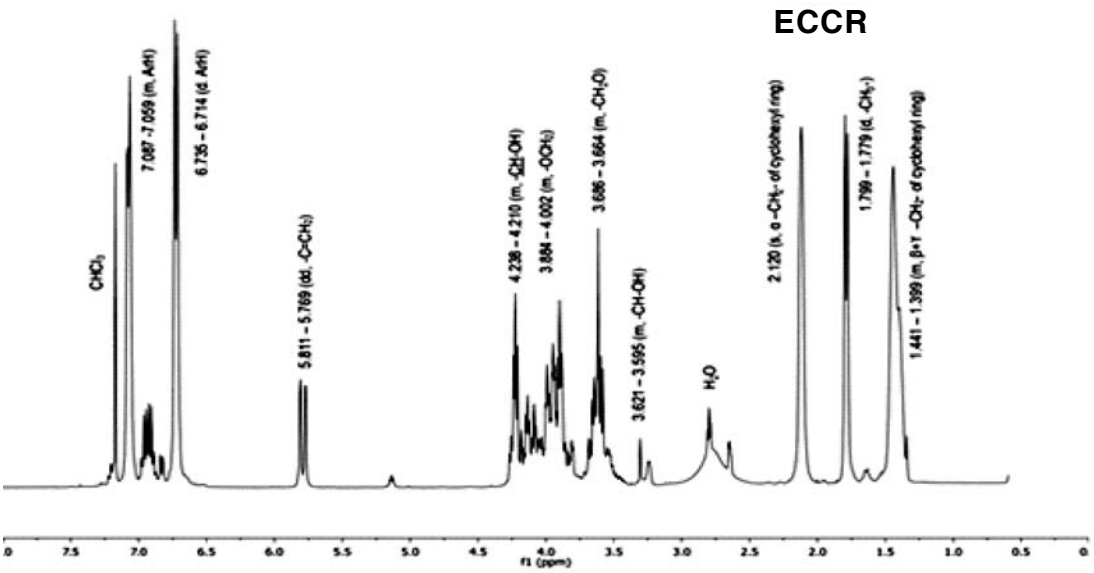

Fig. 2. ^{1}H NMR ($CDCl_3$) spectrum of ECCR.

Thermal Analysis

A DSC thermogram of ECCR is presented in Fig. 3. A small and broad endothermic transition peak at 103°C is assigned as the release of residual trapped water. A broad and strong endothermic transition at 229°C is assigned as melting followed by thermal polymerization of ECCR. The onset of thermal degradation of cured ECCR is supported by an endothermic transition at 300°C and it is confirmed by its TG curve (Fig. 4).

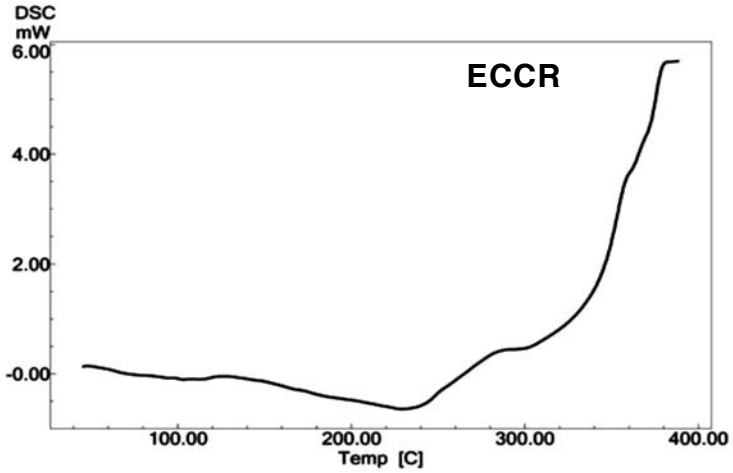

Fig. 3. DSC thermogram of ECCR at 10°C min^{-1} heating rate in a nitrogen atmosphere.

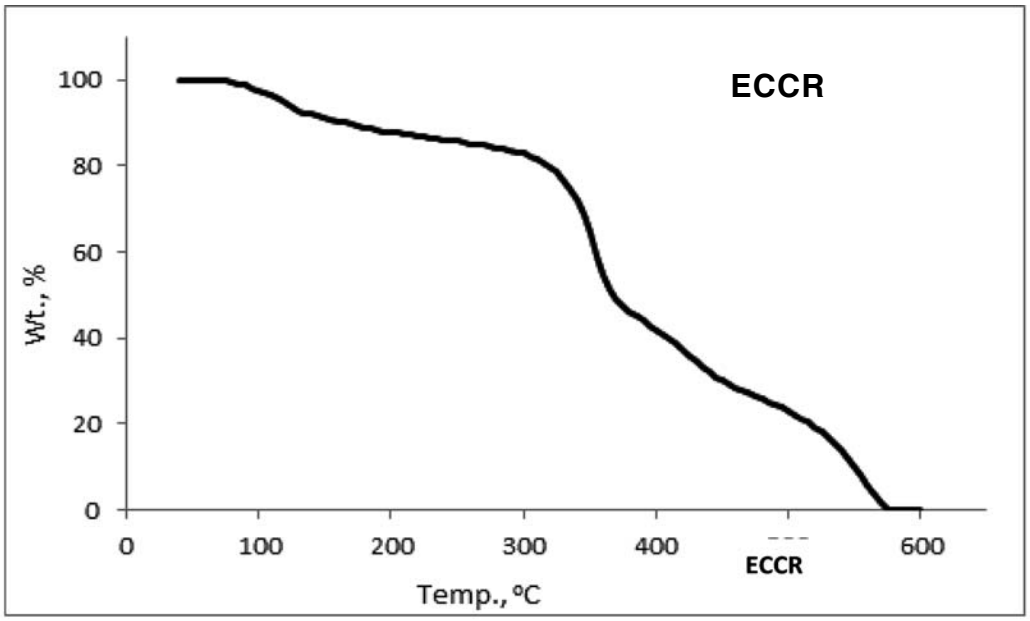

Fig. 4. TG thermogram of ECCR at 10 °C min^{-1} heating rate in a nitrogen atmosphere

From Fig. 4, it is observed that ECCR is thermally stable up to 320°C and follows three-step degradation kinetics. A small weight loss of up to about 100-110°C is due to the release of entrapped water. Initial decomposition temperature (T_o), decomposition range, the temperature of maximum weight loss (T_{max}), and % weight loss involved in each step are reported in Table 3.

Associated kinetic parameters namely energy of activation (Ea), frequency factor (A), and order of degradation reaction (n) were determined according to the Anderson-Freeman method [2]:

$$\Delta ln\frac{dw}{dt} = n\Delta W - \left(\frac{E_a}{R}\right)\Delta\left(\frac{1}{T}\right) \quad (1)$$

$$A = \frac{E_a\beta}{RT^2}\, e^{E_a/RT} \quad (2)$$

$$\Delta S^* = \mathrm{R}\ln\frac{\mathrm{Ah}}{\mathrm{kT}} \quad (3)$$

Where dw/dt is the rate of decomposition, W is the active mass, β is the heating rate, R is

TABLE 3: Thermal data and kinetic parameters of ECCR

T_0, °C	Decomp. Range, °C	T_{max}, °C	Wt. loss, %	E_a, kJ mol^{-1}	n	A, s^{-1}	ΔS*, JK^{-1} mol^{-1}	R^2
320	320-375	375	32.2	196.2	0.89	4.27 X 10^{27}	282.7	0.969
	400-450	450	1.9	99.8	0.46	1.74 X 10^{10}	-51.9	0.966
	505-580	580	22.3	182.9	0.48	1.47 X 10^{15}	40.2	0.991

the gas constant, h is Planck's constant, T is temperature, and k is the Boltzmann constant. The entropy change ΔS^* was determined at the corresponding T_{max}. The least-squares values of the above-mentioned parameters along with regression coefficients (R^2) are reported in Table 3. From Fig. 4 and Table 3, it is noted that the first step followed first-order degradation kinetics, while the second and third steps followed one-half-order degradation kinetics. The E_a values of the first (196.2 $kJmol^{-1}$) and third (182.9 $kJmol^{-1}$) degradation steps are almost doubled that of the second step degradation (99.8 $kJmol^{-1}$). High E_a values of the first-step and third-step degradation kinetics indicated the rigid nature of ECCR and thermally crosslinked resin. By theory, the A values of the first and third steps are observed higher than the second step. The ΔS^* values of the first and third steps are large and positive, while it is large and negative for the second step. The positive and large values of ΔS^* indicated that the transition states are more disorderly states than the initial states, while the negative and large magnitude of ΔS^* indicated a more orderly transition state of the second step.

Ether and ester linkages, as well as side substituents in the resins, are weak points in the resin molecules and selective degradation starts from such weak linkages. The side substituent C-C bonds are less thermally stable than main chain C-C bonds. The selective degradation leads to a variety of reactions namely rearrangement, crosslinking, branching, recombination, etc., and may degrade at elevated temperatures with the evolution of different hydrocarbons depending upon the structure of the materials under investigation.

Mechanical and Electrical Properties

The knowledge of the mechanical and electrical properties of composites is very important for their various applications in our routine life. We have exploited the new matrix material ECCR and reinforced it with jute, glass, and jute-natural fibers for possible industrial applications. The derived tensile strength, flexural strength, electric strength, and volume resistivity of J-ECCR, G-ECCR, and J-B/SC/CO/WH/GN-ECCR are presented in Table 4, from which it is inferred that J-ECCR and G-ECCR showed fairly good tensile strength. The flexural strength of J-ECCR is deceased slightly more than its tensile strength, while the flexural strength of G-ECCR is lowered by three times its tensile strength, which indicates the brittle and rigid nature of the composites. The sandwich composites (J-B/SC/CO/WH/GN-ECCR) showed poor tensile strength and improved stiffness (flexural strength). Relatively poor tensile strength of J-ECCR, G-ECCR, and sandwich composites may also be due to the different nature of matrix and reinforcements, poor interfacial adhesion, and brittle and rigid nature of the composites besides many more factors. In sandwich composites, natural fibers are randomly oriented and as a consequence, stress transfer from matrix to fibers is discontinuous resulting in a lowering in tensile strength. The sandwich materials caused overall improved stiffness of the composites. The tensile and flexural strengths of jute and its sandwich composites of bisphenol-C epoxy methacrylate[13] (J-EBCMAS and J-B/SC/CO/WH/GN-EBCMAS) are found much better than J-ECCR, and J-B/SC/CO/WH/GN-ECCRS. This fact may be due to the different natures of ECCR and EBCMAS matrix materials.

Observed mechanical properties of the composites indicated lightweight low load-bearing housing application at the time of natural calamities.

From Table 4, it is clear that J-ECCR, G-ECCR, and J-B/SC/CO/WH/GN-ECCR displayed poor electric strength and fairly good volume resistivity due to the brittle, rigid, polar, and hydrophilic nature of ECCR as well as poor interfacial bonding of these composites besides many more factors. The sandwich composites showed almost identical electric strength and were 1.3 to 1.5 times lower than J-ECCR. The mechanical and electrical properties of the composites can be improved by the use of a compatibilizer, fiber surface modification, filler, fiber loading, etc. The electric strength and volume resistivity of jute and its sandwich composites of bisphenol-C epoxy methacrylate[13] (J-EBCMAS and J-B/SC/CO/WH/GN-EBCMAS) have practically identical trends with J-ECCR, and J-B/SC/CO/WH/GN-ECCR, which indicated no much polarity difference between ECCR and EBCMAS. The fairly good volume resistivity of the composites indicated their usefulness as electrically insulating materials but do not sustain at very high voltages.

TABLE 4: Mechanical and electrical properties of the composites

Composite	Tensile strength, MPa	Flexural strength, MPa	Electric strength, kV mm^{-1}	Volume resistivity, ohm-cm
J- ECCR	14.4	13.8	1.8	4.5×10^{12}
G-ECCR	206.4	65.5	2.2	4.8×10^{13}
J-B- ECCR	7.4	12.8	1.2	3.1×10^{12}
J-SC- ECCR	5.5	14.5	1.3	2.6×10^{12}
J-CO- ECCR	2.5	9.3	1.4	5.1×10^{12}
J-WH- ECCR	7.0	13.6	1.4	4.0×10^{12}
J-GN- ECCR	5.3	15.6	1.3	2.4×10^{12}

Water Absorption

The knowledge of the moisture tendency of different materials is a must for their applications in humid environments. Natural fibers and resin used in the present study are hydrophilic. The materials made out of them are prone to moisture-sensitive so it is essential to know moisture absorption tendency in different environmental conditions. Assuming unidimensional Fickian diffusivity in the composites, the water absorption tendency of J-ECCR and G-ECCR was carried out in the water, 10% aqueous NaCl and 10% aqueous HCl at 35°C as well as in boiling water by mass change method. The % water absorbed by the composites was determined according to the following Eq. 4:

$$\mathbf{M} = \frac{\mathbf{W_m} - \mathbf{W_d}}{\mathbf{W_d}} \mathbf{x100} \qquad (4)$$

Where M = % water absorbed, W_m = mass of the moist sample, and W_d = mass of the dry sample. The water absorption curves in different environmental conditions for J-ECCR and G-ECCR are presented in Figs 5 and 6, respectively from which, it is observed that the % water absorbed by the composites is increased up to the equilibrium state with time and then remained practically constant. The % equilibrium water content and equilibrium time for J-ECCR and G-ECCR in three different environments are reported in Table 5. From Table 5, it is inferred that the composites have a high water absorption tendency and relatively

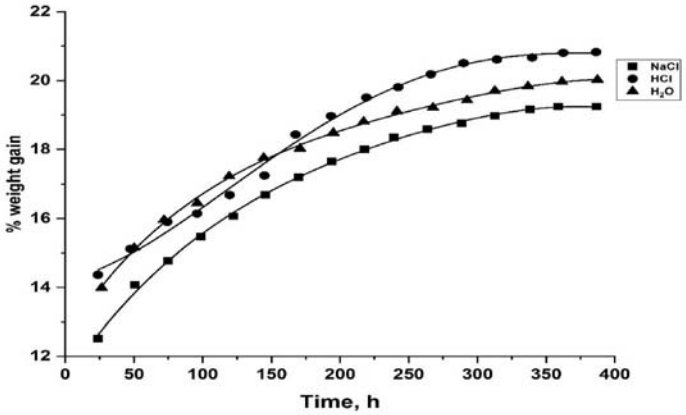

Fig. 5. The plots of percent weight gain against time for J-ECCR in 10% aq. HCl, 10% aq. NaCl and H_2O at 35°C.

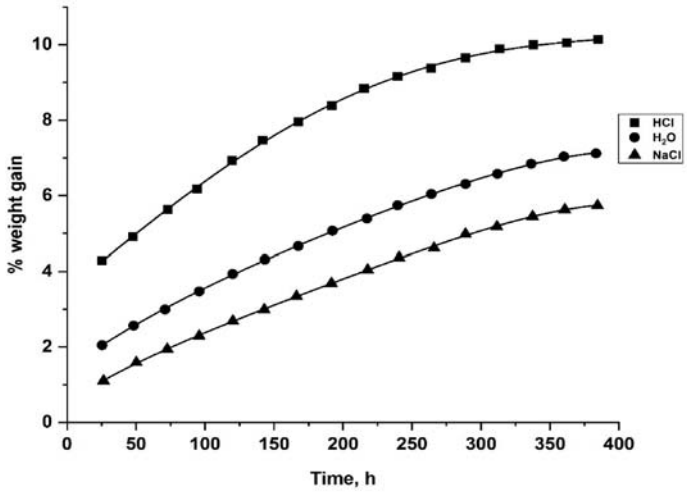

Fig. 6. The plots of percent weight gain against time for G-ECCR in 10% aq. HCl, 10% aq. NaCl and H_2O at 35°C.

longer equilibrium time. Observed water absorption trends in J-ECCR and G-ECCR are HCl > H_2O > NaCl. High water absorption in both composites is mainly due to hydrophilic hydroxyl groups present in the natural fibers and ECCR matrix material. In the case of J-ECCR, a somewhat longer equilibrium time is observed in the water medium (312 h), while it is the same in NaCl and HCl media (288 h). In G-ECCR equilibrium time is the same in all three media (288 h). The nature of the strong electrolytes has affected water structure (polymeric) with the formation of solvated ionic atmospheres, which ultimately affected water absorption and diffusivity tendency in the composites.

TABLE 5: Water uptake and diffusivity data of composites at 35°C

Composite	Eq. water content, %			Eq. time, h			Diffusivity,10^{-13}, m^2s^{-1}			Eq. water content, %
	H_2O	10% NaCl	10% HCl	H_2O	10% NaCl	10% HCl	H_2O	10% NaCl	10% HCl	Boiling water
J-ECCR	19.7	18.8	20.6	312	288	288	9.6	12.5	10.0	22.2
G-ECCR	6.4	5.0	9.6	288	288	288	5.3	5.3	5.5	7.8

The diffusivity of water molecules in J-ECCR and G-ECCR was determined according to the following Eqs. 5 and 6:

$$\mathbf{M} = \frac{\mathbf{4M_m}}{\mathbf{h}}\sqrt{\frac{\mathbf{t}}{\boldsymbol{\pi}}}\sqrt{\mathbf{D_x}} \qquad (5)$$

$$D_x = \pi\left(\frac{h}{4M_m}\right)^2 (Slope)^2 \qquad (6)$$

Where M= % water absorbed at time t, M_m = equilibrium water content, D_x = diffusivity, t = time (second), and h = sample thickness (m). The diffusivity of water in the composites was determined by determining the initial slopes of M vs $\sqrt{t}$ curves and are reported in Table 5. Diffusivity in different sandwich composites is reported in Table 5. The diffusivity of water in the composites depends upon temperature, environmental conditions, the type and nature of the constituents of the composite, and the nature of the electrolytes. The observed diffusivity trend in J-ECCR is NaCl > HCl > H_2O, while for G-ECCR, it is HCl > NaCl = H_2O. In electrolytic solutions, solvated ionic sizes are different and hence affect the diffusivity. The smaller the size of the solvated ions higher the diffusivity[17-19]. Water absorption occurs through capillary action and continues up to saturation point and then free water occupies the voids present in the composites. Due to our limitations, we could not determine void contents in the composites. The absorbed water results in swelling, blistering, cracking, and plasticization of the polymers and fibers and may cause degradation, delamination, void formation, etc. and thereby deterioration of the mechanical properties of the materials under investigation. The swelling, cracking, and blistering result in high water absorption, while degradation leads to the leaching of small molecules and hence a decrease in mass.

Water Absorption in Boiling Water

To understand the effect of temperature on water absorption and hydrolytic stability, the composites were tested in boiling water at intervals of 1 h till limiting values were established. The water absorption curves for J-ECCR and G-ECCR are shown in Fig. 7. The limiting water absorption in the composites is achieved after 4 h, and it is somewhat higher than at 35°C. This fact is probably due to the facts discussed in the previous section. Increasing temperature caused 78 (J-ECCR) and 72 (G-ECCR) times reduction in achieving saturation points. Thus, both the composites showed high water absorption tendency and excellent hydrolytic stability against different reagents, and even in boiling water signifying their utility in harsh environmental conditions as well as elevated temperatures.

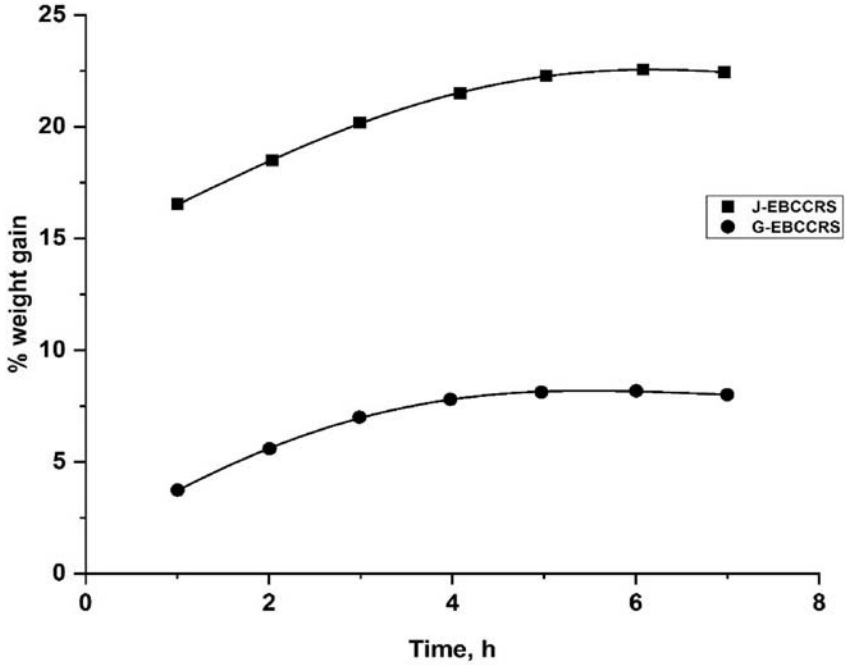

Fig. 7. The plots of percent weight gain against time for J-ECCR and G-ECCR in boiling water.

CONCLUSIONS

A novel bisphenol-C epoxy crotonate resin has been synthesized and characterized by various techniques. The resin is used for preparing its fiber-reinforced composites. The composites showed moderate to poor tensile and flexural strengths, electric strength, and fairly good volume resistivity. Jute- and Glass-ECCR composites have high water absorption tendencies and excellent hydrolytic stability against harsh environmental conditions.

ACKNOWLEDGMENTS

The authors are thankful to the director, ERDA Vadodara for electrical testing and the Council of Scientific and Industrial Research for major research project funding (01(2440)/10/EMR-II, Dt. 28-12-10).

References

1. F. R. Jones, and J. P. Foreman. (2015). The response of aerospace composites to temperature and humidity. In Polymer Composites in the Aerospace Industry. Woodhead Publishing, 335-369
2. T. Xie, W. Liu, T. Chen, and R. Qiu. (2015). Mechanical and thermal properties of hemp fiber-unsaturated polyester composites toughened by butyl methacrylate. *BioResources,* 10: 2744-2754.
3. W. Tahri, Z.Abdollahnejad, J. Mendes, F. Pacheco-Torgal, and J. Barroso de Aguiar. (2017). Cost efficiency and resistance to chemical attack of a fly ash geopolymeric mortar versus epoxy resin and acrylic paint coatings. *Eur. J. Environ. Civ. Eng.* 21: 555-571.
4. W. Dehas, M. Guessoum, A. Douibi, J. A. Jofre-Reche, and J. M. Martin-Martinez. (2018). Thermal, mechanical, and viscoelastic properties of recycled poly(ethylene terephthalate) fiber reinforced unsaturated polyester composites. *Polym. Compos.* 39: 1682-1693.
5. S. M. Razavi, N. Dehghanpour, S. J. Ahmadi, and M. Rajabi Hamaneh. (2015). Thermal, mechanical, and corrosion resistance properties of vinyl ester/clay nanocomposites for the matrix of carbon fiber reinforced composites exposed to an electron beam. *J. Appl. Polym. Sci.* 132. https://doi.org/10.1002/app.42393.
6. Y. Zhang, Y. Li, V. K. Thakur, Z. Gao, J. Gu, and M. R. Kessler. (2018). High-performance thermosets with tailored properties derived from methacrylated eugenol and epoxy-based vinyl ester. Polym. Int. 67: 544-549.
7. J. P. Patel, and P. H. Parsania. (2018). Biodegradable and biocompatible polymer composites, properties and applications characterization, testing and reinforcing materials of biodegradable composites, Woodhead Publishing, Elsevier, Duxford, United Kingdom, 55-79.
8. Shen Lu, Li Yinwen, Zheng Jian, Lu Mangeng, Wu. Kun. (2015). Modified epoxy acrylate resin for photocurable temporary protective coatings. *Prog. Org. Coat.* 89: 17-25
9. J. D. Thanki, and P. H. Parsania. (2016). Synthesis and characterization of epoxy methacrylate of (E)-1, 3-bis (4-hydroxyphenyl) prop-2-en-1-one and its jute/glass composites. *World Scientific News,* 42: 182-196.
10. J. D. Thanki, and P. H. Parsania. (2016). Synthesis and physicochemical study of epoxy methacrylate of 9,9'-bis(4-hydroxy phenyl) anthrone-10 and its jute and glass composites. *J. Polym. Mater.* 33: 305-317.
11. P. D. Desai, and R. N. Jagtap. (2022). Synthesis of ultraviolet curable bisphenol-based epoxy acrylates and comparative study on its physicochemical properties. *J. Appl. Polym. Sci.* 139. doi.org/10.1002/app.52022.
12. Yi Wang, Zhonghua Vhen, and Fei Yu. Preparation of epoxy-acrylic latex based on bisphenol F epoxy resin. J. Macromol. Sci. Part A: Pure and Appl. Chem. 55 (2018) doi.org/10.1080/10601325.2017.1410065
13. J. V. Patel, J. P. Patel, R. D., and P. H. Parsania. (2015). Mechanical and electrical properties of jute-biomass-styrenated methacrylate epoxy resin sandwich composites. *J. Sci. Indus. Res.* 74: 577-581.
14. J. V. Patel, J. P. Patel, R. D. Bhatt, and P. H. Parsania. (2016). Filled and unfilled glass/jute-epoxy methacrylate of 1,1'-bis(4-hydroxyphenyl) cyclohexane composites: Mechanical and electrical properties, *Indian J. Chem. Technol.* 23:153-157.

15. R. D. Bhatt, J. P. Patel, and P. H. Parsania. (2021). Potential comparison of montmorillonite filled and unfilled epoxy methacrylate of bisphenol-C-glass/ jute/treated jute and hybrid composites. *World Scientific News* 158: 227-246.

16. P. H. Parsania, and J. P. Patel. (2021). Synthesis and evaluation of some physical properties of epoxy methacrylate of bisphenol C: a comparative study with commercial resin Aeropol 7105. *Polym. Bul.* 78: 7355-7367.

17. R. D. Bhatt, J. P. Patel, and P. H. Parsania. (2021). Glass/Biofibers/Epoxy methacrylate of bisphenol-C sandwich composites: Comparative mechanical and electrical properties and chemical resistance. *J. Polym. Mater.* 38: 71-87.

18. R. D. Bhatt, J. P. Patel, and P. H. Parsania. (2022). Fabrication and comparative properties of sustainable epoxy methacrylate of bisphenol-C-Jute/Treated Jute-Natural fibers sandwich composites: Part-I. *J. Polym. Mater.* 39: 205-221.

19. R. D. Bhatt, J. P. Patel, and P. H. Parsania. (2022). Fabrication and comparative properties of sustainable epoxy methacrylate of bisphenol-C-Jute/Treated Jute-Natural fibers sandwich composites: Part-II. *J. Polym. Mater.* 39: 223-239.

20. D. A. Anderson, and E. S. Freeman. (1964). The kinetics of the thermal degradation of polystyrene and polyethylene. *Polym. Sci.* 54: 253–260.

Received: 12-01-2023

Accepted: 25-06-2023